Physics of the Earth and Planetary Interiors xxx (2016) xxx–xxx

Contents lists available at ScienceDirect

Physics of the Earth and Planetary Interiors

journal homepage: www.elsevier.com/locate/pepi

Near-field radiated wave field may help to understand the style of the supershear transition of dynamic ruptures

Andrea Bizzarri [a,*], Chao Liu [b]

[a] Istituto Nazionale di Geofisica e Vulcanologia, Sezione di Bologna, Via Donato Creti, 12, 40128 Bologna, Italy
[b] Department of Earth Sciences, University of Oxford, South Parks Road, OX1 3AN Oxford, UK

ARTICLE INFO

Article history:
Received 28 September 2015
Received in revised form 24 May 2016
Accepted 24 May 2016
Available online xxxx

Keywords:
Supershear earthquakes
Ground motions
Wave propagation
Dynamic models of faults
Computational seismology

ABSTRACT

Supershear earthquakes are known to leave special signatures in the signals on the fault (fault slip velocity, dynamic traction evolution, energy flux, etc.) and in the ground motions. Moreover, two different styles of supershear transition have been identified; in the direct transition (DT) mechanism the rupture speed continuously increases from the sub-Rayleigh to the terminal speed of *P* waves, while in the mother–daughter (MD) mechanism a forbidden zone of rupture speed exists and a secondary pseudo-rupture is generated ahead of the primary rupture front. Here we found that the off-fault signals (wavefields) generated by these two mechanisms are rather different, in that the MD case contains an enhanced trailing Rayleigh field, which has very low amplitudes (or it is even practically absent) in the DT case, and possess higher frequency content. Therefore, we show that it is possible to distinguish the style of the supershear transition from the records of real earthquakes. In particular, basing on the results of our numerical simulations, we can conclude that the Denali, Alaska, earthquake was basically controlled by a classical MD mechanism.

1. Introduction

It is well known that supershear earthquakes (namely, dynamic ruptures propagating with a rupture speed greater than that of the *S* waves of the medium surrounding the seismic source, v_S) possess some features that differentiate them from subshear events. Indeed, supershear earthquakes emit a Mach cone which is fully coherent at some distance from the fault (Bernard and Baumont, 2005) and which has enhanced high frequencies that can overwhelm those arising from stress heterogeneity (Spudich and Frazer, 1984; Bernard and Baumont, 2005; Bizzarri et al., 2010). Moreover, they can radiate a wave front having less geometric spreading than that radiated from subshear events (Bernard and Baumont, 2005; Bizzarri and Spudich, 2008). They also emit Rayleigh Mach waves which do not attenuate with distance from the fault trace (Dunham and Bhat, 2008). Additionally, ground motions of supershear events are richer in high frequencies (Bizzarri et al., 2010) and they extend widely in the direction perpendicular to the fault trace, with a predominance of the fault-parallel component of the particle velocity (Aagaard and Heaton, 2004). Finally, supershear earthquakes tend to enhance rake rotation (Bizzarri and Cocco, 2005; Bizzarri and Das, 2012); this can have consequences in the formulation of analytical expression of the slip-dependent constitutive models (Bizzarri, 2014b). All these features have relevant practical implications and this is the reason of an increasing interest in studying supershear earthquakes and, in general, to infer the rupture speed of dynamic events (Das, 2007). An up-to-date list of real-world earthquakes that have been identified as supershear can be found in Bizzarri (2014; his Table I). Indeed, there are also some attempts to relate supershear events to seismic hazard (e.g., Andrews, 2010 among others).

Within the range of supershear rupture speeds, there are two rather different supershear transition mechanisms (Geubelle and Kubair, 2001; Liu et al., 2014; see also Festa and Vilotte, 2006); one is the direct transition (DT thereinafter) and the other one is the mother–daughter (MD thereinafter) transition (see also Dunham, 2007; Liu and Lapusta, 2008; Lu et al., 2009). In particular, Liu et al. (2014) found that for weak faults (namely, for relatively small values of the strength parameter S ($\sim 0.38 \leqslant S \leqslant \sim 0.72$)) the ruptures penetrate the previously considered forbidden zone of rupture speed (between Rayleigh speed, v_R, and v_S) through the direct transition mechanism. As well known, $S \underset{\mathrm{df}}{=} \frac{\tau_u - \tau_0}{\tau_0 - \tau_f} = \frac{\Delta\tau_0}{\Delta\tau_d}$ expresses the degree of instability of a fault, in that a low value of S identifies an unstable fault, over which a rupture

* Corresponding author. Tel.: +39 051 4151432; fax: +39 051 4151499.
E-mail addresses: andrea.bizzarri@ingv.it (A. Bizzarri), Chao.Liu@earth.ox.ac.uk (C. Liu).

http://dx.doi.org/10.1016/j.pepi.2016.05.013
0031-9201/

with relevant stress drop is expected. The strength parameter, which in fact is the ratio between the strength excess and the dynamic stress drop, has been first introduced by Das and Aki (1977a,b). The importance of the S parameter resides in the fact that it discriminates between supershear and sub-Rayleigh propagation regimes, depending of the fact that the value of S is below or above, respectively, a critical value, which in turn depends on the dimensionality of the problem (2-D or 3-D problem; see Dunham, 2007). Indeed, the rupture speed (v_r, the measure of the velocity at which the rupture propagates on the fault surface) continuously increases from sub-Rayleigh speeds to the terminal speed of P waves, v_P, without any jump, contrarily to the previous believe from Andrews (1976); the rupture crosses the forbidden and the unstable zones through a rapid acceleration. In this case, the energy flux at the rupture front undergoes a sharp but monotonic increase, including the velocity range $v_R < v_r < v_S$ (Bizzarri, 2013) that is forbidden in the 2-D, steady-state, singular cracks (Broberg, 1999). On the other hand, for stronger faults (namely, when $\sim 0.76 \leqslant S \leqslant \sim 1.3$) there is a peak in the shear stress field (i.e., a stress concentration) which travels ahead of the main (mother) rupture front and causes the birth of a secondary (daughter) pseudo-rupture is ahead of mother front. While the latter asymptotically approaches v_R, the former starts to propagate already in the supershear regime and finally can reach v_P. In this case, the MD mechanism, the forbidden zone does really exist and the rupture speed experiences a jump from the sub-Rayleigh regime to the supershear one. Correspondingly, the energy flux at the rupture front exhibits a sharp peak during the coalescence of the main and the daughter rupture fronts (Geubelle and Kubair, 2001). This MD regime has been explored in the above-mentioned, pioneering paper by Andrews (1976)—S was 0.8 in that case; see his Fig. 3—and in fact becomes the epitome of the supershear rupture propagation. Indeed, the large (nearly complete, with the very few, recent exceptions mentioned above) subsequent literature on this subject assumed that the MD mechanism was the unique behavior of supershear ruptures.

The distinction between these two styles has been obtained by computing the rupture speed v_r and looking whether it fails within the forbidden zone (as for the DT mechanism) or not (as for the MD mechanism). v_r is computed by using the two-points central difference scheme, in which in the fault node i is expressed as it follows:

$$v_r(i) = \frac{2\Delta x}{t_r(i+1) - t_r(i-1)} \tag{1}$$

where Δx is the spatial sampling (i.e., the discretization along the direction of the propagation of the rupture) and t_r is the rupture time of the node i, which in turn is defined as the first instant at which the fault slip velocity in i exceeds the threshold value of v_l = 0.01 m/s (Bizzarri and Das, 2012). Moreover, the distinction between the two styles of supershear transition has been also made by looking whether the cohesive zone (where the stress is released on the fault) exhibits its so-called bifurcation, i.e., if there is the birth of a secondary (daughter) rupture front ahead from the primary (or mother) front. Due to the numerical nature of the problem, it is virtually impossible to find an *exact*, *arbitrarily accurate* value which distinguishes the two regimes, and this is the reason why Liu et al. (2014) gave the value "~0.72" as upper bound for S in the DT mechanism and the value of "~0.76" as lower bound for the MD mechanism.

Since the styles of the supershear transition (DT and MD mechanisms) have rather different signatures on the fault surface, as elucidated by Liu et al. (2014), it is natural to ask whether the off-fault behavior is also different, i.e., whether the signals recorded out of the fault contain some special features and can therefore be used to infer what kind of transition mechanism is operating on a fault. This is the main goal of the present study.

2. Method

We solve the elastodynamic problem for a 2-D, pure in-plane (mode II) fault geometry and always including inertia. Namely, we solve the fundamental elastodynamic equation for faults (i.e., the Newton's second law of dynamic for rigid bodies), which, neglecting body forces (such as electric and magnetic forces, gravity, etc.), reads

$$\rho \ddot{u}_i = \sigma_{ij,j} \tag{2}$$

in which ρ is the cubic mass density of the medium surrounding the fault, $\mathbf{u}$ is the fault slip (formally, the displacement discontinuity), σ_{ij} are the stress tensor components and repeated index are summated (Einstein's convention assumed). Eq. (2) is solved numerically, as described in details in Bizzarri et al. (2001) and in Liu et al. (2014). Here we simply recall that the problem is solved by using a second-order accurate, finite difference scheme, based on triangular grid, with homogeneous mesh. The code is OpenMP-parallelized. The nucleation is imposed in an initialization patch (exactly as in Liu et al., 2014; their Section 2) and then the rupture propagates spontaneously (i.e., without prior-assigned rupture speed) along x_1 (see Fig. 1). For the mode II geometry assumed here, the fault slip is then $((u_1(x_1,t)),0,0)$, since no opening or interpenetration of material is allowed and the solutions only depend, by definition, on the x_1 coordinate. The fault is governed by the classical slip-weakening law, which prescribes a linear decrease of the fault friction with increasing fault slip over the prescribed, characteristic distance d_0:

$$\tau = \begin{cases} \left[\mu_u - (\mu_u - \mu_f)\frac{u}{d_0}\right]\sigma_n^{eff} & , u < d_0 \\ \mu_f \sigma_n^{eff} & , u \geqslant d_0 \end{cases} \tag{3}$$

In Eq. (3) $\mu_u \sigma_n^{eff} = \tau_u$ is the upper yield stress and $\mu_f \sigma_n^{eff} = \tau_f$ is the residual level (σ_n^{eff} is the effective normal stress, which is assumed to be constant through time in the present work). We

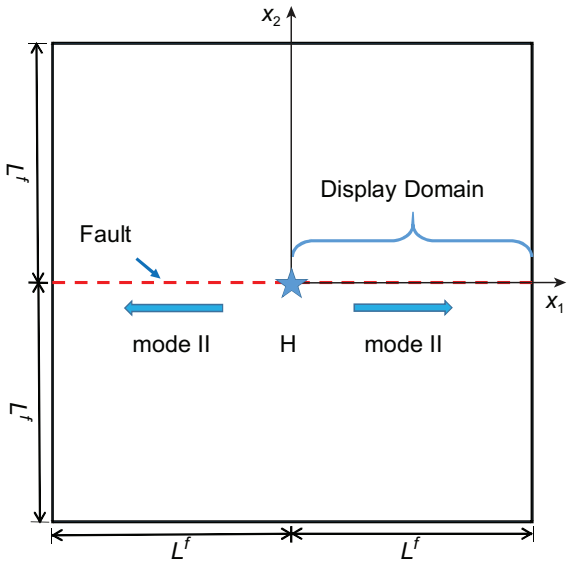

Fig. 1. Geometry of the fault considered in the present study. The dashed line indicates the fault trace. The rupture nucleates at the (imposed) hypocenter H and then propagates bilaterally and spontaneously. Due to the symmetry of the problem, only one half of the fault is considered (as indicated).

Please cite this article in press as: Bizzarri, A., Liu, C. Near-field radiated wave field may help to understand the style of the supershear transition of dynamic ruptures. Phys. Earth Planet. In. (2016), http://dx.doi.org/10.1016/j.pepi.2016.05.013